# The high velocity, high adiabat, “Bigfoot” campaign and tests of indirect-drive implosion scaling

D. T. Casey, C. A. Thomas, K. L. Baker, B. K. Spears, M. Hohenberger, S. F. Khan, R. C. Nora, C. R. Weber, D. T. Woods, O. A. Hurricane, D. A. Callahan, R. L. Berger, J. L. Milovich, P. K. Patel, T. Ma, A. Pak, L. R. Benedetti, M. Millot, C. Jarrott, O. L. Landen, R. M. Bionta, B. J. MacGowan, D. J. Strozzi, M. Stadermann, J. Biener, A. Nikroo, C. S. Goyon, N. Izumi, S. R. Nagel, B. Bachmann, P. L. Volegov, D. N. Fittinghoff, G. P. Grim, C. B. Yeamans, M. Gatu Johnson, J. A. Frenje, N. Rice, C. Kong, J. Crippen, J. Jaquez, K. Kangas, and C. Wild

Citation: Physics of Plasmas **25**, 056308 (2018); doi: 10.1063/1.5019741

View online: https://doi.org/10.1063/1.5019741

View Table of Contents: http://aip.scitation.org/toc/php/25/5

Published by the American Institute of Physics

# The high velocity, high adiabat, "Bigfoot" campaign and tests of indirect-drive implosion scaling

D. T. Casey,[1,a)] C. A. Thomas,[1] K. L. Baker,[1] B. K. Spears,[1] M. Hohenberger,[1] S. F. Khan,[1] R. C. Nora,[1] C. R. Weber,[1] D. T. Woods,[1] O. A. Hurricane,[1] D. A. Callahan,[1] R. L. Berger,[1] J. L. Milovich,[1] P. K. Patel,[1] T. Ma,[1] A. Pak,[1] L. R. Benedetti,[1] M. Millot,[1] C. Jarrott,[1] O. L. Landen,[1] R. M. Bionta,[1] B. J. MacGowan,[1] D. J. Strozzi,[1] M. Stadermann,[1] J. Biener,[1] A. Nikroo,[1] C. S. Goyon,[1] N. Izumi,[1] S. R. Nagel,[1] B. Bachmann,[1] P. L. Volegov,[2] D. N. Fittinghoff,[1] G. P. Grim,[1] C. B. Yeamans,[1] M. Gatu Johnson,[3] J. A. Frenje,[3] N. Rice,[4] C. Kong,[4] J. Crippen,[4] J. Jaquez,[4] K. Kangas,[4] and C. Wild[5]
[1]*Lawrence Livermore National Laboratory, Livermore, California 94550, USA*
[2]*Los Alamos National Laboratory, Los Alamos, New Mexico 87545, USA*
[3]*Massachusetts Institute of Technology, Cambridge, Massachusetts 02139, USA*
[4]*General Atomics, San Diego, California 92121, USA*
[5]*Diamond Materials GmbH, Freiburg 79108, Germany*

(Received 15 December 2017; accepted 25 February 2018; published online 30 March 2018)

The Bigfoot approach is to intentionally trade off high convergence, and therefore areal-density, in favor of high implosion velocity and good coupling between the laser, hohlraum, shell, and hotspot. This results in a short laser pulse that improves hohlraum symmetry and predictability, while the reduced compression reduces hydrodynamic instability growth. The results thus far include demonstrated low-mode symmetry control at two different hohlraum geometries (5.75 mm and 5.4 mm diameters) and at two different target scales (5.4 mm and 6.0 mm hohlraum diameters) spanning 300–405 TW in laser power and 0.8–1.6 MJ in laser energy. Additionally, by carefully scaling the 5.4 mm design to 6.0 mm, an increase in target scale of 13%, equivalent to 40% increase in laser energy, has been demonstrated. *Published by AIP Publishing.* https://doi.org/10.1063/1.5019741

## I. INTRODUCTION

To achieve hotspot ignition, inertial confinement fusion (ICF) implosions must produce high hotspot internal energy inertially confined by a dense shell of DT fuel.[1,2] To accomplish this, experiments at the National Ignition Facility (NIF)[3] are designed to achieve high peak implosion velocity, good energy coupling between the incident laser, the hohlraum, and the imploding shell, and finally the hotspot at stagnation, which is inertially confined by a high areal-density shell. However, experiments have shown that achieving these simultaneously is extremely challenging, partly because of inherent tradeoffs between these three interrelated requirements. For example, it takes time to launch a series of carefully sequenced shocks to maintain a low shell adiabat (defined as $\alpha = P/P\text{cold}$, where $P$ is the DT fuel pressure at peak velocity, and $P\text{cold}$ is the minimum pressure at 1000 g/cm$^3$ from the DT equation of state) required to achieve high areal density.[4] This temporal constraint competes with hohlraum plasma closure, inhibiting the beam propagation, which in turn makes the implosion symmetry more difficult to predict and control. Also, sharp density gradients in the capsule shell and high convergence ratios are subject to more hydrodynamic instability growth that can destroy the integrity of the shell and inject higher-Z ablator mass into the hotspot radiating hotspot energy away. In fact, experiments during the National Ignition Campaign (NIC) demonstrated record high areal-density but also showed that pushing those implosions in velocity could result in worse performance and lower yield due to Rayleigh-Taylor breakup of the inflight implosion and mix of the ablator material into the high spot.[5–8]

In the absence of 2D and 3D effects like hohlraum asymmetries and hydrodynamic instabilities, the yield of a 1D implosion in the absence of energy deposition from the alpha particles ($Y^{1D}_{no-\alpha}$) should scale strongly with implosion velocity ($v$), adiabat ($\alpha$), system scale (S), and the ablation pressure ($p_{abl}$)[9–11] as

$$Y^{1D}_{no-\alpha} \propto \frac{p_{abl}^{0.8}\, v^{7.7}\, S^{4.4}}{\alpha^{1.8}}. \quad (1)$$

Experimental performance during the NIC did not follow this scaling with velocity and adiabat suggesting that strong 2D and 3D effects were dominating 1D behavior, which was later confirmed experimentally.[6,8,12,13]

The Bigfoot approach is to trade off high convergence and areal-density, for conditions that are favorable for controlling hohlraum symmetry and hydrodynamic instabilities. The aim is improving predictability, while leveraging high velocity, potentially enabling high yields at high adiabat ($\alpha \sim 4$–5).

The results of this campaign so far are reviewed in this paper. Section II will review the overall target design strategy, and Sec. III will show experiments demonstrating low-mode symmetry control at two different hohlraum geometries (5.75 mm and 5.4 mm diameters). Section IV will demonstrate the impact of a change of target scale (5.4 mm and 6.0 mm hohlraum diameters) spanning 300–405 TW in laser power and 0.8–1.6 MJ in laser energy. Hydrodynamic instability growth from engineering features like the capsule

Note: Paper GI3 2, Bull. Am. Phys. Soc. **62**, 112 (2017).
[a)]Invited speaker.

fill tube are currently thought to be a major factor in reducing performance compared to calculations. Section IV will present some evidence supporting this hypothesis as well as other asymmetries whose origin is still under investigation. Section V will put this work into context of prior experiments, present plans going forward, and summarize.

## II. DESIGN STRATEGY

The initial choices of the Bigfoot design were focused around improving experiment predictability, while maintaining flexibility to test implosions physics by stressing the platform in velocity, scale, and adiabat in subsequent experimental series. A few examples of initial design choices, described briefly in this section and by Thomas *et al.*,[14] are splitting of the outer cones and individual beams within outer quads, a short pulse high adiabat target design where the first 2 shocks merge at the ice/ablator interface, and an intermediate hohlraum gas fill, all of which are designed to reach high velocity.[15]

Controlling hohlraum symmetry is extremely challenging because of the inherent tradeoffs between hohlraum physics, such as beam propagation and laser plasma interactions (LPIs), and 1D capsule physics, such as adiabat. For example, because of the expanding hohlraum wall and capsule ablator plasmas, propagation of the laser beams to the hohlraum waist is increasingly inhibited at later times, thereby reducing equatorial capsule drive and making symmetry control of the implosion difficult to maintain. In addition to using a hohlraum gas fill of $\sim$1 mg/cm$^3$ of $^4$He to tamper wall motion, a novel solution to this problem implemented during the NIC was to rely on cross-beam energy transfer between the inner and outer cones[16] to increase the drive on the hohlraum waist while maintaining a balanced use of the NIF laser (all beams at approximately the same power). A tradeoff of that approach is that the laser-plasma interaction (LPI) process that drives this energy transfer between the inner and outer cones depends on the detailed plasma conditions and is a complex time dependent process that is challenging to calculate (because of uncertainties in time-dependent plasma conditions, empirical saturation parameters, etc.).

A possible solution to this problem tested here is to utilize a short laser pulse shape that accelerates the capsule while inner beam propagation is still maintained and easier to predict. Figure 1 shows the Bigfoot pulse shape compared to a low foot (LF) pulse shape. An intermediate hohlraum 0.3 mg/cm$^3$ helium gas fill was utilized to help slow the inward expansion of the hohlraum wall, while also avoiding the reduced energy-coupling and LPI issues like stimulated Raman scattering (SRS) observed in previous experiments.[17] The first two steps in the laser pulse launch shocks that are designed to merge near the ice/ablator interface making the pulse shape especially short compared with traditional designs that minimize adiabat by merger near the ice inner surface. Furthermore, the design does not use hard-to-predict cross-beam energy transfer to balance the hohlraum energy deposition. A tradeoff to these features is that it is more difficult to maintain a low fuel $\alpha$ because of typically faster and stronger shocks. However, the 1D benefits of low adiabat,

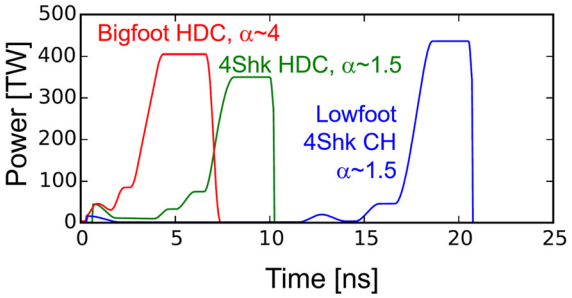


FIG. 1. Total laser power as a function of time for the high $\alpha \sim 4.0$ HDC Bigfoot (red curve), low $\alpha \sim 1.5$ HDC, and low $\alpha \sim 1.5$ CH lowfoot (blue curve) plotted as a function of time. The much shorter Bigfoot pulse shape results in less hohlraum filling by the time of peak power for the same hohlraum-gas-fill.

such as increased convergence, compression, and shell areal-density may be greatly reduced if the hohlraum drive introduces strong 2D and 3D asymmetries, or hydrodynamic instabilities that can grow and degrade the implosion. Moreover, the integrated Bigfoot design results in lower ablation front growth factors than similar designs at lower adiabat,[18] and the shock merger at the ice/ablator interface helps reduce the Atwood number resulting in improved interface stability. Also, the shock merger at the ice/ablator interface causes increased ablation of the ice inner surface during hotspot formation resulting in increased ablative stabilization of the ice inner surface interface. Simulations predict that this configuration is therefore more robust to high-mode ice surface roughness. Nevertheless, the three step laser design can be modified such that the 1st and 2nd shocks are retimed to collide later in the ice or at the ice inner surface by simply extending the foot of the laser pulse shape. Importantly, this means that the $\alpha \sim 4$ pulse shape can be walked toward lower $\alpha$ by a small change to the laser pulse shape.

Current models[11,19] predict a closure of the hohlraum wall where the outer cone is incident (referred to as the "gold bubble"), which is dependent on the outer cone laser intensity at early time (picket). The relationship is such that higher intensities in the early time laser pulse cause the gold bubble to grow faster, reducing the period where the inner cone path is clear, making propagation to the waist of the hohlraum more challenging later in time. Therefore, reducing the intensity on the wall can slow the growth of the gold bubble. This motivated splitting the incident laser spots in the outer cone by separating the 44° and 50° cones by $\sim$1 mm at the hohlraum wall as well as individual beams in the quads. This also reduces intensity modulation on the hohlraum wall, and thereby the seed for Rayleigh-Taylor instability on the gold bubble expanding into the hohlraum-fill-gas and capsule blow-off plasmas.[20] Additionally, reducing the incident laser power is anticipated to reduce the amount of backscattered laser light from LPI.

## III. EXPERIMENTS AT REDUCED SCALE (0.8×)

### A. Experimental configuration

Experiments at reduced physical scale have substantially reduced costs in terms of laser optics damage because of

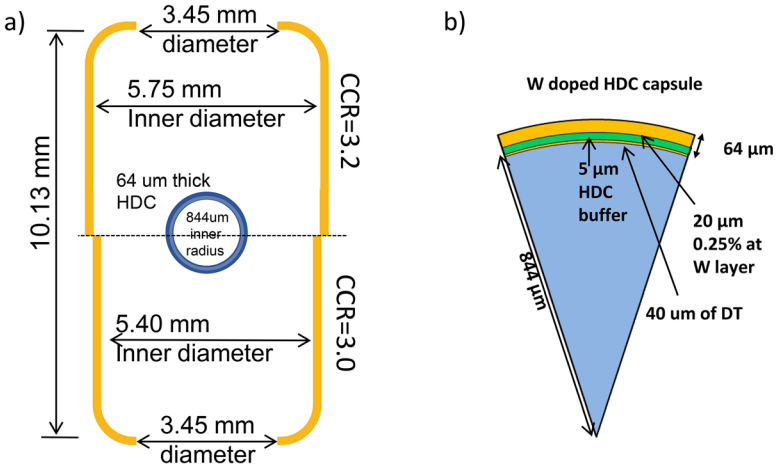


FIG. 2. (a) Schematic of the two hohlraum diameters (5.75 mm and 5.4 mm) or case-to-capsule ratios (CCRs) that were tested at 0.8× scale with the same hohlraum length and LEH. (b) Illustration of the capsule dimensions that were the same in the two hohlraum configurations.

reduced energy and power requirements. Therefore, initial experiments testing these new integrated concepts were designed to be 80% smaller in physical scale (or 0.8×) than those designed to use the full laser energy/power performance. This resulted in initial tests at about ∼1/2 the total laser energy (0.8–1 MJ) and ∼2/3 the total laser power (300–320 TW) of designs intended to utilize the full NIF laser (∼1.8 MJ and 500 TW).

The first series of experiments[15] were designed to test overall low mode P2 shape control and assess the impact of LPI. These experiments used a 5.75 mm diameter Au hohlraum and a 844 $\mu$m inner radius high-density carbon (HDC)[21–28] capsule with a wall thickness of 64 $\mu$m. While most HDC capsules were W doped, a few undoped shells were also tested. W-doped HDC capsules consisted of a 5 $\mu$m thick layer of undoped HDC on shell inside, followed by a 20 $\mu$m HDC layer doped with ∼0.25 at. % W, followed by a 36 $\mu$m undoped HDC layer.[29] Both undoped and W-doped HDC shells had a fine grained texture with grain sizes ranging from 1 to 10 $\mu$m. However, for the outermost 3 $\mu$m, the deposition conditions were changed to grow nanocrystalline HDC which is easier to polish and thus improves the surface finish. All relevant dimensions are shown in Fig. 2.

### B. Experimental observations

A series of $D^3He$ (or $DT^3He$) gas-filled, symcap,[30] experiments were performed to assess LPI and implosion symmetry from the hotspot x-ray self-emission images at ≈10 keV obtained using time-integrated image plate detectors and gated x-ray framing cameras.[31,32] The hotspot self-emission is analyzed using Legendre mode decomposition. Here, mode 2 (P2) symmetry is controlled using the inner and outer beam cone power balance, characterized by cone fraction (CF), or the ratio of the inner power divided by the total power. P4 symmetry is controlled using the geometric considerations. Figure 3(a) shows the measured P2 from hotspot self-emission as a function of the CF at peak power (which is held constant through peak power), for the two hohlraum diameters 5.75 mm and 5.4 mm. Note that the smaller 5.4 mm diameter hohlraum is predicted to have a somewhat stronger drive for the same laser energy than the 5.75 mm hohlraum because of its smaller cavity volume. A clear correlation between P2 and CF demonstrates good symmetry control. The decrease in core P2 between 5.75 mm and 5.4 mm hohlraums is principally because the outer cone beams are intercepted earlier by the wall, thus subtending a smaller angle with respect to the capsule pole. Figure 3(b) shows simulated P2 vs experiment and the comparison shows excellent predictability (RMS ∼5 $\mu$m) of P2 mode symmetry for these two hohlraum geometries.[15]

The experiments also showed high laser energy coupling to the hohlraum (∼99%) with relatively little observed stimulated Brillouin scattering (SBS) and SRS.[15] At higher intensities/powers (∼320–340 TW), SBS increased toward the end of the pulse on the 50° outer beams while remaining peaked in the center of the pulse for the inner 23° beams.

## IV. TESTS OF HYDRO-EQUIVALENCE

### A. Hydro-equivalence scaling considerations and experimental design

Understanding how ICF systems change with scale has long been of interest[2,33–37] since the cost of experiments (i.e., size of the facility) is a strong function of scale. Indeed, even in a fixed facility such as the NIF, the cost of operating the laser increases at high power and energy due to damage to the optics and the costs of refurbishment. Furthermore, as experiments are extrapolated from smaller to larger scale, it is important that these extrapolations are accurate and tested as well as possible.

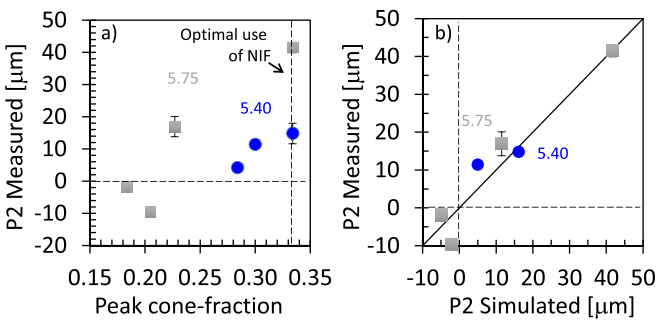


FIG. 3. (a) Plot of the experimentally x-ray P2 as a function of cone fraction (CF) for 0.8× scale experiments. The clear trends and agreement with simulation show good hotspot symmetry control at two CCRs. (b) Simulation vs experiment x-ray hotspot image P2.

The interested reader is referred to a recent publication by Nora *et al.*[35] for a review of current theory of hydro-equivalence ICF systems with a focus on direct drive experiments, but which remains valid in many respects for how an indirectly driven implosion will respond to changes of scale. Briefly, one expects similar hydro-dynamic behavior under a change in scale S (scale multiplication factor), if the relevant length scales, such as capsule radius, thickness, hohlraum radius, height, and LEH diameter, are all scaled by S. This means that all volumes and masses are changed by $S^3$, laser power is scaled by $S^2$, and laser energy by $S^3$. The system time scales and therefore implosion temporal evolution are stretched or compressed by S. This is expected to produce roughly the same hohlraum radiation temperature (roughly because the hohlraum wall albedo increase in time) and therefore similar ablation pressure and capsule drive. The in-flight aspect ratio, peak implosion velocity, hotspot pressure, shell density, and the stagnation aspect ratio are approximately maintained the same under a change in scale. The shell areal density, hotspot areal density, and confinement, and hence burntime is expected to scale approximately by S, the ion temperature ($T_i$) by $S^{0.2}$ (due to reduced thermal conduction losses), and hence the yield (neglecting alpha heating) is expected to scale by $S^{4.4}$.

Not all aspects of the implosion obey hydrodynamic similarity and so some deviation from hydro-equivalence and corresponding uncertainty from extrapolation to larger or smaller scale should be expected. For example, alpha-heating is not scale-invariant such that larger scale implosions are predicted to benefit more. Other aspects are not expected to scale, such as scale-lengths set by material properties of the hohlraum and capsule materials, such as opacities, particle mean-free paths, and their effect on density and temperature scale-lengths. Some aspects of hydrodynamic instability growth might be expected to scale, but the ablative-stabilization mechanisms (ablation velocities, scale lengths, etc.) do not scale, nor do the seeds for hydrodynamic instabilities such as surface roughnesses, and engineering features like the capsule support tent[38] and the capsule fill tube.[39] Additionally, because the spot sizes as set by phase-plates are kept fixed, the laser spot intensities inside the hohlraum and related LPI processes increase with scale. Therefore, measurements that directly assess the change in performance and other observables are important to help build confidence in how systems scale and how to assess uncertainties.

### B. Experimental configuration at 0.9×

To assess the impact of a change in target scale, the 5.4 mm hohlraum[15] was increased by $S = 0.9/0.8 = 1.125$ to 0.9× scale rather than going to 1.0× outright. The reason is that 0.9× offered more flexibility in terms of laser power on the inner and outer cone and lower risks due to LPI than making a larger initial step. This resulted in a hohlraum inner diameter of 6.00 mm and length of 11.30 mm, an inner capsule radius of 950 $\mu$m, a capsule thickness of 72 $\mu$m, and an LEH diameter of 3.9 mm. Similar to the 0.8× capsule described earlier, the W doped layer in the HDC capsule is recessed 5 $\mu$m from the inner surface but is thicker at 22 $\mu$m thick. Outside of the W doped layer is another 42 $\mu$m of undoped HDC with an additional outermost 3 $\mu$m nanocrystalline HDC layer. To maintain hydrodynamic similarity, the W doped region should have a similar optical-depth (or initial W-doped HDC areal density) but because of target manufacturing realities, the first experiments were 0.13% W and so had lower total optical-depth. Figure 4(a) illustrates the geometry and compares to the 0.8× (5.4 mm) geometry. A scaling of the fill-tube induced perturbation is difficult as it is a combination of radiation-hydrodynamic and geometric seeds.[39] Instead, the capsule fill-tube perturbation was decreased from 10 $\mu$m [Fig. 4(c)] to 5 $\mu$m [Fig. 4(b)] diameter to reduce its seed and overall impact. The resulting laser energy and peak power on target was 1.6 MJ and 405 TW, compared to 1.1 MJ and 320 TW, and all times were stretched by 1.125×. The 0.8× laser pulse requested on shot N161030 [solid black curve in Fig. 4(d)] is compared to a pulse where the laser power is multiplied by $S^2$ and times stretched by S (dashed black curve) and to the requested laser pulse for the 0.9× experiment N170524 (red curve).

### C. Experimental observations

Previous experiments at 0.8× suggested that a case-to-capsule size ratio of ∼3.0 would enable a balanced use of the NIF inner and outer cone powers (CF = 1/3) allowing the next series of experiments to be designed to potentially enable use of the NIF laser at full power ∼500 TW. A series of gas filled experiments tested the CF relationship (shown in Fig. 5) and suggested a near optimum of 33% to maintain P2 symmetry control in the 6.00 mm hohlraum in equivalent layered DT experiments. An offset was observed between the experiments at 0.8× and 0.9× scale in the P2 vs CF relationship, perhaps because of increased intensity on the hohlraum wall leading to faster hohlraum-wall expansion and hohlraum closure at larger scale. Experiments continued to show high coupling (∼98%) with relatively little SRS at 0.9× scale. However, again SBS increased toward the end of the pulse on the 50° outer beams and on the 23° beams (peaking near the center of the pulse) which has been attributed to higher intensities.

A DT layered experiment (N170524) was performed at 0.9× scale to assess the integrated target performance, compared to a close companion at 0.8× scale (N161030). The geometry is identical to that described in Fig. 4 except that an additional 45 $\mu$m of cryogenically frozen DT ice is layered on the inside of the HDC capsule, scaled by S from the 40 $\mu$m of DT ice on N161030. The measured ice roughness figure-of-merit $k_{ice}$ and the effective mode 1 amplitude are summarized in Table I.[40] Experimentally measured P2 from various shots, including the DT layered implosions, are shown as a function of cone fraction in Fig. 5. The layered implosion at 0.9× scale has a slightly more negative P2 symmetry than the corresponding gas-filled implosions because of an expected decrease in velocity due to the increased mass introduced by the DT layer that leads to sampling more of the pole-hot drive later in time with a slower trajectory.

Figure 4(e) shows the delivered (dashed) and requested (solid) laser pulse shapes for N161030 (black) and N170524

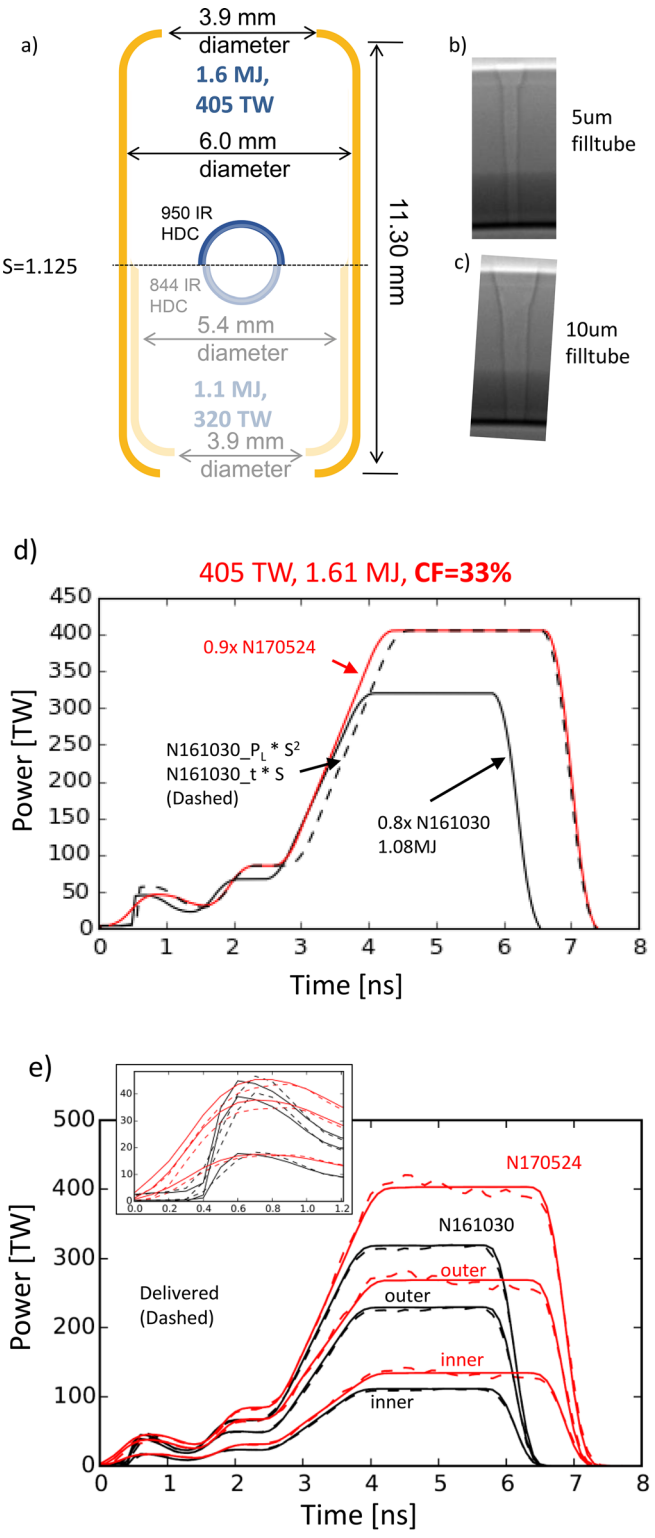


FIG. 4. (a–c) Schematic of hohlraum dimensions for 0.8× (5.40 mm diameter) and 0.9× (6.00 mm diameter experiments. (d) The laser power as a function of time for the 0.8× scale shot N161030 (black curve), exact hydroscale of N161030 to 0.9× (black dashed curve), and the 0.9× shot N170524 (red curve). The target and laser pulse shape were scaled to maintain hydro-equivalence between 1.1 MJ and 1.6 MJ experiments. (e) Requested (solid curve) verse delivered (dashed) laser pulse shapes.

(red). At peak power, the delivery is within request to about ~2% in both cases on both the inner and outer cones. It is more challenging to deliver the lower power parts of the pulse accurately than the peak power portion of the pulse. In

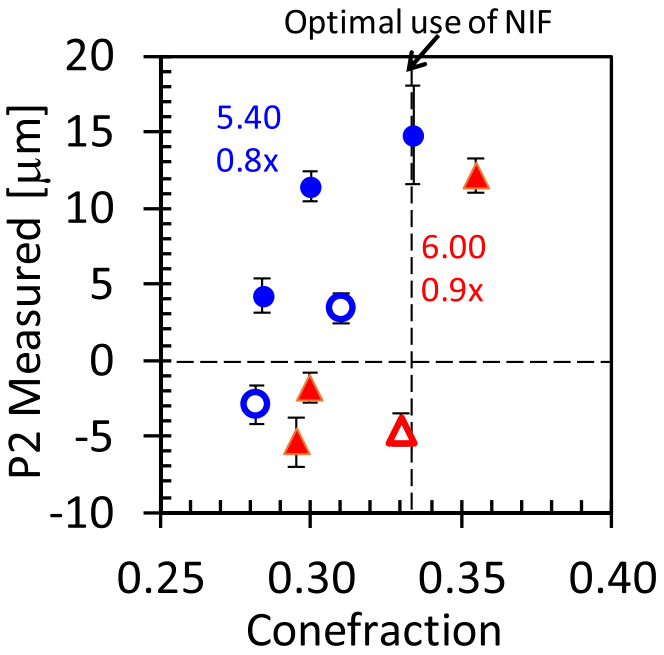


FIG. 5. Plot of the experimentally x-ray P2 as a function of cone fraction for 0.9× scale experiments (red triangles) compared to 0.8× scale (blue circles, 5.4 mm hohlraum). Open symbols are DT experiments, while solid symbols are symcaps. The observed hotspot symmetry behavior is similar at increased scale with a –P2 offset.

this intermediate hohlraum-gas system, the implosion is very sensitive to the picket [zoomed portion of Fig. 4(e)], particularly in the outer cone because of its impact on hohlraum closure dynamics described earlier. On N161030, the picket energy was higher than request on the inner cone by about 6% and on the outer cone higher by about 1% in the picket. This is expected to have little impact. On N170524, both the inner and outer cones were lower by about 8% in the picket. The reduced intensity of the outer cone picket is predicted to reduce the gold bubble expansion and increase the P2 by roughly ~5 um. The trough and second step of the laser pulse are important for fuel adiabat but this implosion system is not very sensitive to their delivery because of the high fuel adiabat.

The overall performance of the N170524 can be assessed by examining the total yield of DT reactions, which was inferred to be $6.2 \pm 0.1 \times 10^{15}$ from the measured neutrons in the 13–15 MeV integral[41] and the down-scattered ratio (DSR) or 10–12 MeV to 13–15 MeV neutron yield ratio. The 13–15 MeV yield, Ti, DSR, BT, and yield-over-clean (YOC), and other relevant metrics are summarized in Table I. The measured yield was ~3.3× larger at 0.9× than observed in N161030 at 0.8×, which is roughly 2× larger than would be anticipated by pure scaling arguments ($S^{4.4}$). This is likely due at least in part to the reduced fill tube diameter, which has been shown[39,42] to reduce the perturbation to the capsule shell and improve implosion performance.[43]

A small increase in performance may also be attributed to an increase in yield amplification due to alpha-heating.[44,45] To infer the alpha-heating contribution to the yield, the ignition threshold factor ($ITFX = (Y_{13-15}/4e15) \times (DSR/0.067)^{2.3}$) can be used.[41] However, ITFX was developed at a

TABLE I. Summary of layered DT experiments and observations. Here $R_{cap}$ is the inner radius of the capsule, $t_{cap}$ is the capsule thickness, $t_{ice}$ is the ice thickness, $k_{ice}$ is the rms ice roughness figure of merit, $\ell_{ice} = 1$ is the effective ice mode one amplitude, $D_H$ is the hohlraum inner diameter, BT is the peak x-ray emission, the P0 measured using the primary neutron image, and YOC is the $(Y_{DT}/Y_{1D})$ where $Y_{1D}$ is calculated from 1D simulations.

| | Capsule parameters | | | | | | Hohlraum parameters | | | | Experimental data | | | | | | |
|---|---|---|---|---|---|---|---|---|---|---|---|---|---|---|---|---|---|
| Shot # | $R_{cap}$ ($\mu$m) | $t_{cap}$ ($\mu$m) | W (%) | $t_{ice}$ ($\mu$m) | $k_{ice}$ ($\mu$m) | $\ell_{ice}=1$ ($\mu$m) | $D_H$ (mm) | $E_{las}$ (MJ) | $P_{las}$ (TW) | $C_F$ (%) | $Y_{13-15}$ $\times 10^{15}$ | DSR % | $T_i$ (keV) | P0 (ns) | BT (ns) | $Y_{DT}$ $\times 10^{15}$ | YOC-1D (%) |
| N160207-002-999 | 844 | 64 | 0.00 | 40 | ~1.3 | 0.20 | 5.75 | 0.81 | 290 | 24 | 0.17 | 1.42 ± 0.1 | 3.21 ± 0.14 | NA | 7.51 | 0.18 | 22 |
| N161030-001-999 | 844 | 64 | 0.25 | 40 | 1.1 | 0.17 | 5.4 | 1.06 | 320 | 28 | 1.67 | 2.88 ± 0.3 | 4.14 ± 0.17 | 24 | 7.23 | 1.87 | 31 |
| N170109-002-999 | 844 | 64 | 0.25 | 40 | 1.4 | 0.42 | 5.4 | 1.151 | 333 | 31 | 2.34 | 2.87± 0.1 | 4.16 ± 0.12 | 22 | 7.25 | 2.63 | 22 |
| N170524-002-999 | 950 | 72 | 0.13 | 45 | 0.8 | 1.60 | 6 | 1.557 | 405 | 33 | 5.55 | 2.78 ± 0.1 | 4.45 ± 0.12 | 28 | 7.90 | 6.20 | 20 |

certain scale and with a corresponding DT fuel mass ($M_{DT\text{-}rev5} = 171\ \mu g$) and so comparison of different scales and initial fuel masses requires care. Recent work[44,46–48] has shown that the yield (experimental yield with alpha heating) should be normalized by the DT fuel mass, if fuel thickness scales with size, because of the re-expression of the ignition metrics in terms of yield rather than temperature. This comes from the balance of hotspot internal energy to shell kinetic energy used in expressing yield in terms of $T_i$ and $M_{DT}$.[49] Also, since the fuel is 36% thinner for the Bigfoot implosions relative to most lower $\alpha$ designs, we expect the stagnated fuel areal density to be of order 36% smaller at a given in-flight adiabat. The remaining mass of the ablator may also play some small role in how these models should be applied, but in the following we will neglect its impact. We can therefore define a target scale parameter ($S_M$) in terms of the initial DT fuel mass relative to that used in the development of ITFX or $S_M = (M_{DT}/M_{DT\text{-}rev5})^{1/3}$. While very similar to the Bigfoot target scales defined earlier, $S_M$ enables cross-platform comparisons by accounting for differences in Bigfoot initial ice thickness and inner capsule diameter. Now reapplying the procedure outlined in Betti *et al.* 2015[44] but instead using $ITFX_{\alpha\text{-}on}/S_M{}^3$ to infer the yield amplification results in an inferred increase in alpha heating of about ~1.2× increase inferred at larger scale. This follows from N161030 $ITFX_{\alpha\text{-}on} = 0.060$ and $ITFX_{\alpha\text{-}on}/S_M{}^3 = 0.12$ implying a yield amplification of ~1.36×, while for N170524 $ITFX_{\alpha\text{-}on} = 0.18$ and $ITFX_{\alpha\text{-}on}/S_M{}^3 = 0.25$ implying a yield amplification of ~1.58×.

Other surrogacy issues may also play a role, for example, the reduced W dopant in the capsule is predicted to ablate slightly faster and may lead to less remaining mass (in fact N170524 is inferred to be going ~10 km/s faster, resulting in ~1.2× increase from velocity), and the possibility of more preheat at the ice/ablator interface leading to worse interface stability.

The observed primary neutron images[50,51] are shown in Fig. 6(a), for both the 0.8× and 0.9× experiments. As previously noted, the hotspot size and $\rho$R are expected to increase with ~S. Indeed, the primary neutron P0 is larger by 17% ± 13% not far from expected, and the hotspot shape is relatively similar, despite the change in hohlraum case-to-capsule ratio (CCR) defined as hohlraum radius over capsule radius and CF. The down-scattered neutron image, which consists of primary neutrons that have scattered off the dense DT into the 6–12 MeV binned image, is shown for both shots in Fig. 6(b). The down-scattered image is also larger at increased scale by 36% ± 13%. Interestingly, despite the larger down-scattered image, the total DSR as shown in Fig. 7(a), which is the ratio of 10–12 MeV/13–15 MeV neutrons and is a measure of areal density, is about the same. However, the uncertainty on the 0.8× experiment is larger than the expected change with scale. Note that the relationship between DSR and total hotspot and shell $\rho$R depends on the implosion geometry at stagnation. Interestingly, the Bigfoot implosion is designed to increase the hotspot to shell $\rho$R ratio, which is expected to decrease the neutron path lengths through scattering material. This effectively lowers the observed DSR for the same

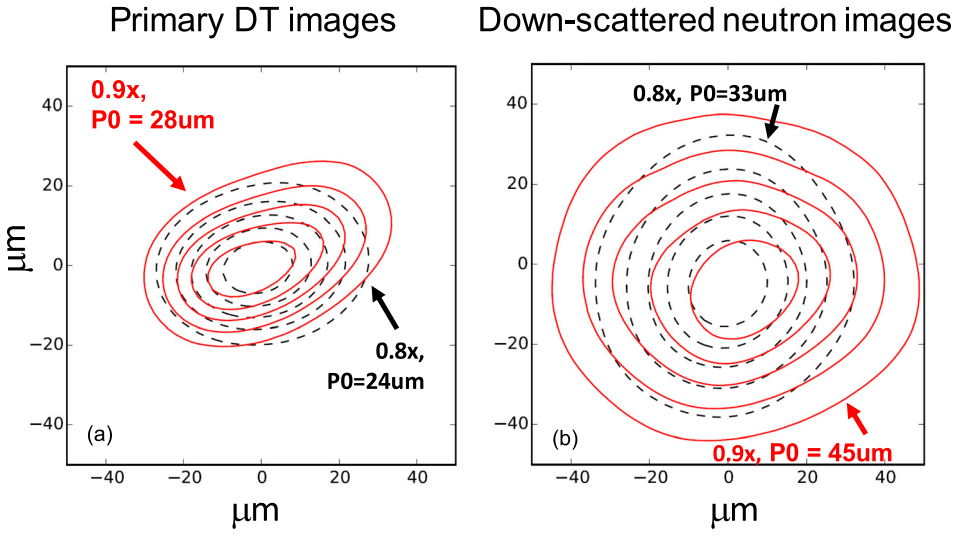


FIG. 6. Observed neutron images from 0.9× (red contours) and 0.8× (black dashed contours) experiments, where the outer contour is 17% of the peak intensity and each inward contour is an integer multiple higher contour. (a) The primary 13–15 MeV image was ~17% larger with increased scale. (b) The 6–12 MeV image is sensitive to the fuel is ~36% larger with increased scale.

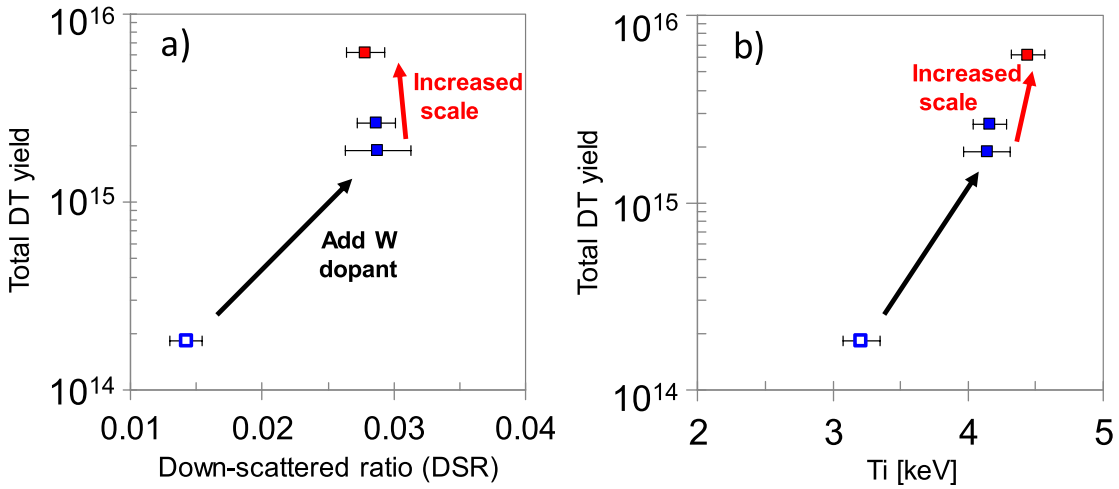


FIG. 7. (a) DT yield (total) plotted as function of down-scattered ratio (DSR). (b) DT yield (total) plotted as function of ion temperature (Ti). Increased scale resulted in higher yield, slightly higher temperatures, and comparable DSR.

total $\rho$R. The yield is plotted as function Ti in Fig. 7(b). Increasing scale resulted in about 5% increase in temperature, which is about twice what might be expected from pure scaling arguments but not significantly outside uncertainty. Nevertheless, increased alpha-heating and the reduced fill-tube perturbation might be expected to lead to slightly higher Ti.

The yield as a function of peak power is plotted in Fig. 8(a). As is evident, increasing power results in increased observed yield, as do increased scale and capsule dopant. Increased total laser power also has a strong impact on implosion velocity. The yield as a function of inferred implosion velocity is shown in Fig. 8(b). The data show a strong relationship with implosion velocity although the uncertainties are too large to constrain the relationship until more data have been obtained. For comparison, the expected relationship in the absence of strong-alpha heating, i.e., $\sim v^8$, is also shown.

Observations of the compressed DT shell are made with the flange neutron activation detector suite (FNADs),[52] the neutron time of flight detectors (nTOFs),[53] and the magnetic recoil spectrometer (MRS).[54] The observed FNAD data for the 0.9× and two 0.8× shots are shown along with low-mode fits in Fig. 9(a) as a function of NIF angular coordinates, theta and phi. The FNAD data measure the unscattered neutron yield, which is sensitive to path integrated areal-density ($\rho$L) via neutron attenuation. Using neutron attenuation cross-sections $Y/Y_{avg} \approx 1 - 0.2\times\delta\rho L$ (g/cm$^2$). However, the exact relationship to $\delta\rho$R requires a model of the source and scattering material. Nevertheless, the data indicate significant shell anisotropies (blue areas are high $\rho$R, and red low $\rho$R). The observed DSRs are plotted on the same angular coordinate. The observed DSRs show a similar high $\rho$R region on N161030 centered around the 315° azimuth and low $\rho$R region around 180°. The DSRs appear relatively isotropic on N170524 and N170109 despite observed FNAD asymmetries, likely because of a lack of angular coverage of the DSR spectrometers. Interestingly, all three implosions have a low $\rho$R region centered around 90°.

Polar x-ray self-emission for N161030 and a surrogate D$^3$He gas-fill implosion N161006 is shown in Fig. 10. The images where obtained using HGXD detectors filtered to detect photon energies >8 keV have an integration time of 100 ps, and with pinhole/magnification that results in a resolution ~10 um. In both the gas-filled and layered experiments, a prominent feature is observed 100 ps before bang-time (peak x-ray emission), which is seeded by the capsule fill-tube and likely the tip of a perturbation consisting of both W and C. Later in time, the perturbation is harder to distinguish (especially in the case of the layered shot) from the hotspot emission but is still present.

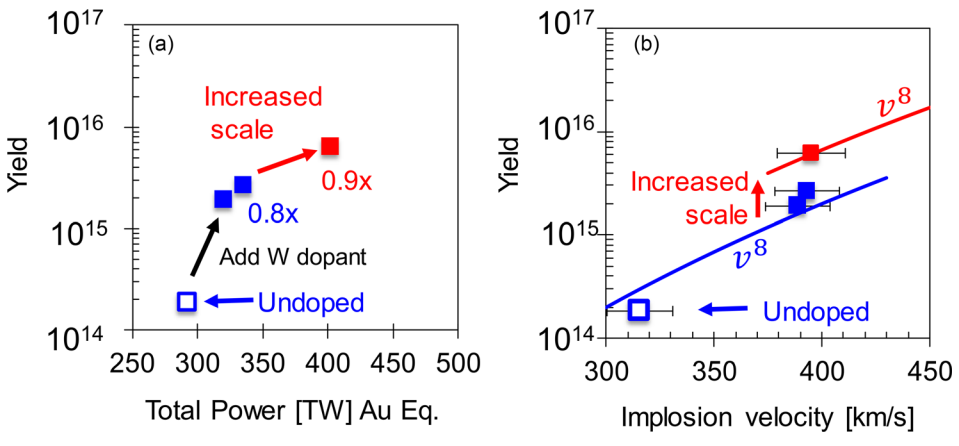


FIG. 8. (a) Total yield as a function of laser power. 0.8× experiments are shown in blue and 0.9× in red. (b) Total yield as a function of inferred velocity. Implosion performance improved with capsule dopant, laser power, implosion velocity, and scale.

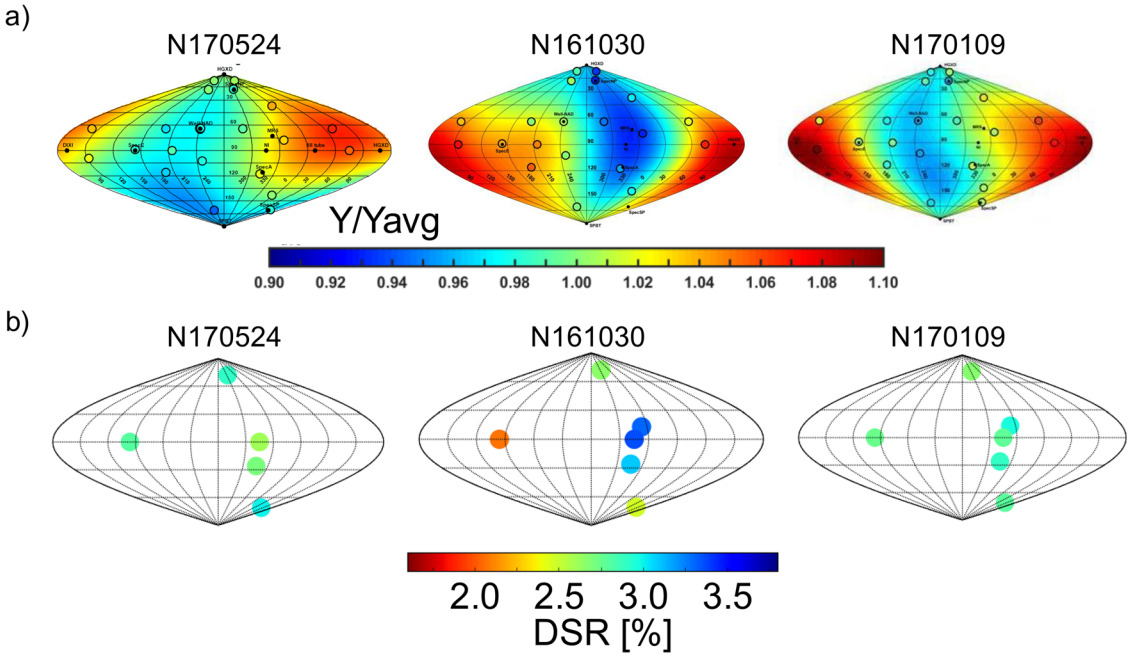


FIG. 9. (a) FNAD data observed and fit on three Bigfoot DT implosions. (b) Observed DSRs from the same experiments and plotted on the same angular map as the FNAD data.

Figure 11(a) shows the FNAD data for N161030, already shown in Fig. 9(a) but now projected looking downward from the north pole. The observed DSRs are shown in Fig. 11(b) looking downward from the pole. Figure 11(c) shows the x-ray self-emission from the pole (as already shown in Fig. 10) but now with the angles relevant to several features highlighted and with additional late time x-ray images showing the outgoing shock and late time hotspot emission. Interestingly, early before bangtime the fill tube perturbation is clearly visible and well aligned with the fill-tube's initial location azimuth of ∼7°. At bangtime, the fill-tube perturbation becomes harder to distinguish from the hotspot self-emission. After bangtime the outgoing shock radiates as it traverses through the remaining and infalling fuel and HDC ablator. The hotspot self-emission continues but now is offset from the outgoing shock centroid. This is consistent with higher drive from an azimuth of 320° leading to more fuel compression at 320° as observed in both the DSRs and FNAD diagnostics and bulk hot spot flow towards 140° as is seen. However, a source for this hypothetical drive imbalance has not yet been found. It is also possible that other low mode perturbations could be significant such as capsule defects or low mode ice asymetries, while the high adiabat Bigfoot drive is predicted to be more stable to high mode capsule and ice perturbations, it is predicted to be vulnerable to low mode perturbations. It is possible that the hotspot is venting through the observed low $\rho$R region at 140° at late time, but again the source of this $\rho$R perturbation is still not understood.

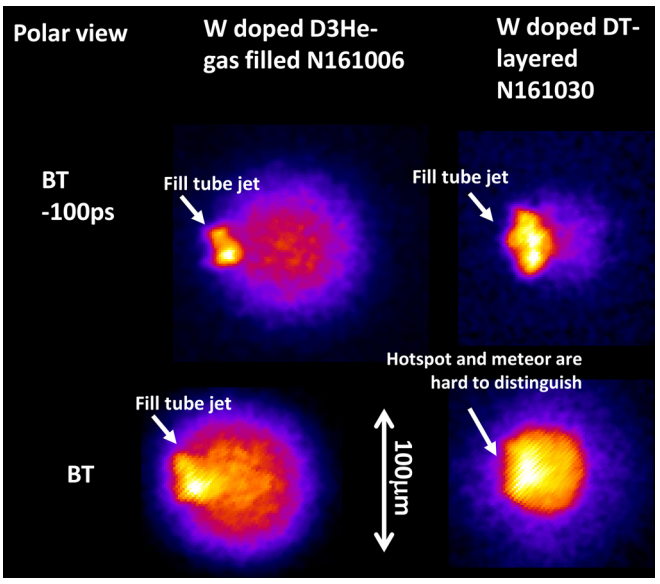


FIG. 10. Observed x-ray self-emission images from the pole from a $D^3He$ gas filled symcap (left) and a DT layered implosion (right). Both implosion platforms show a prominent emission feature due to the fill tube induced perturbation.

## V. SUMMARY AND FUTURE WORK

To put this work into context with prior experiments, we plot progress against the ignition metric ITFX,[41] already introduced, or equivalently plot the total yield as a function of measured DSR. As noted earlier, to compare to contours of alpha-heating with different target scales, the total yield should be normalized by $M_{DT}$ or $S_M{}^3$. Figure 12 shows the Yield/$S_M{}^3$ as a function of DSR. By using the alpha heating relationships discussed earlier, Fig. 12 also shows contours of yield amplification. The Bigfoot experiment (red squares) are compared to Lowfoot (LF), Highfoot (HF), and Adiabat Shaped (AS), and other HDC experiments.[10,24,27,45,55–57] The other HDC experiments are designed for lower adiabat ($\alpha \sim 2.5$) at larger CCR than the Bigfoot experiments described herein, and ongoing experiments are exploring a

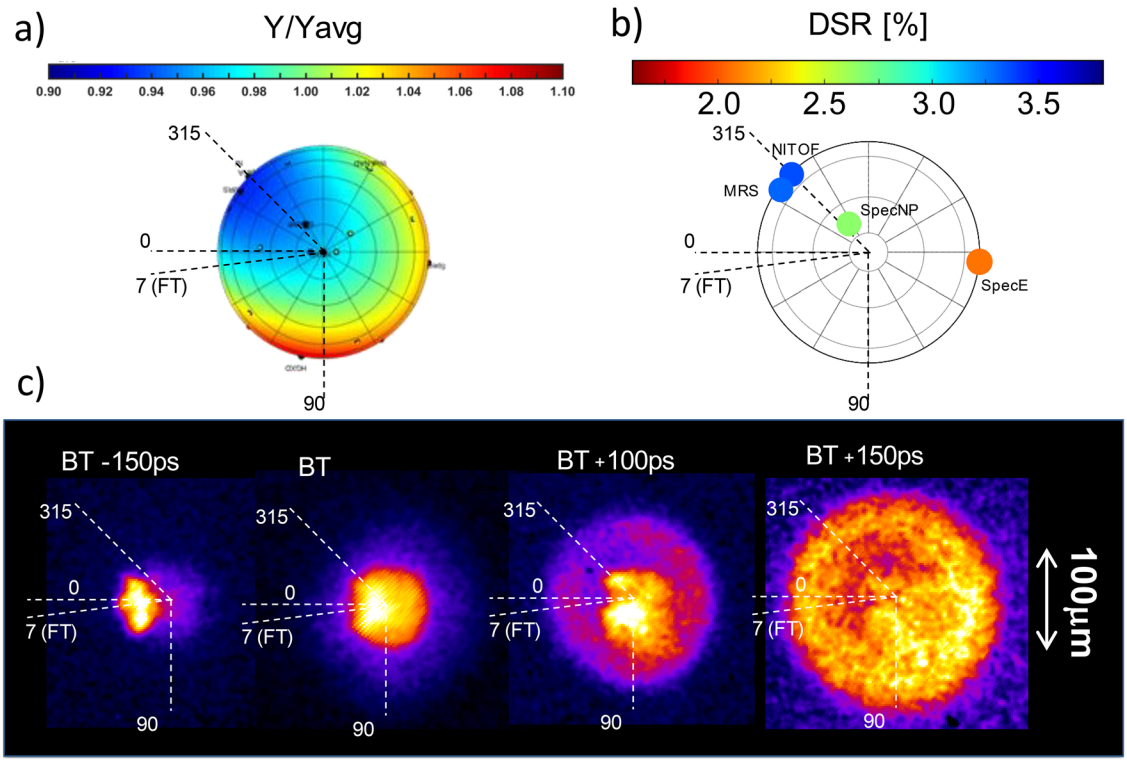


FIG. 11. Asymmetries observed from the capsule pole. (a) FNAD distribution showing large M1 asymmetry about the ~140–320 axis. (b) Observed DSRs from the neutron spectrometers which corroborate the asymmetry observed in FNADs. (c) X-ray emission before bangtime shows a strong feature centered about ~7°, while late time emission appears increased toward region where the fuel is thinner.

910 inner radius capsule with a 6.2 mm inner radius hohlraum.[58] This comparison illustrates the tradeoffs and advantages of the Bigfoot platform as high-yield has been achieved at lower DSRs (due to high adiabat and a proportionately 36% thinner fuel layer) than many previous experiments. Also illustrated nicely is the stepwise progression of increasing velocity and scale to observe the impact on performance. As previously noted, increases in velocity and scale attempted so far have resulted in higher yield and overall performance. The strategy for experiments in the future is to continue to higher velocities up to ~450 km/s at 0.9× scale and to decrease the adiabat from ~4 to ~2.5 to observe the impact on performance with a simple change to the laser pulse shape.

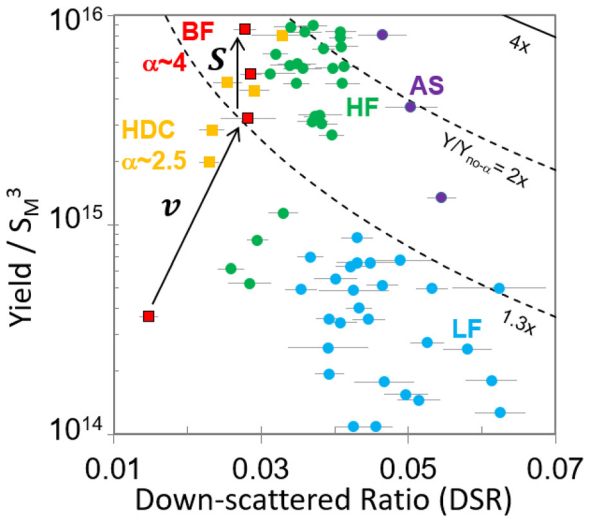


FIG. 12. Yield normalized by $S_M^3$, defined here as $S_M^3=M_{DT}/M_{DT\text{-}rev5}$ as a function of DSR and compared to alpha heating contours. The Bigfoot strategy is to approach from a high adiabat, low DSR, part of the parameter space and slowly increase scale, velocity, and finally DSR to test the impact on overall performance.

In summary, the Bigfoot platform has been tested at 0.8× and 0.9× scale to better understand ICF implosion predictability and performance with short pulse shapes and at high adiabat. So far, hotspot symmetry control has been tested in three different hohlraums geometries at two scales with a short (5.5–7 ns) laser pulse shape and intermediate (0.3 mg/cm$^3$) hohlraum gas fill. A change in target scale has been demonstrated that helps to constrain models of hydro-dynamic equivalence that are important for extrapolating performance to higher laser powers and energies. This implosion data has already been useful in comparing the three ablators[18,59] and will be extremely valuable in developing future implosion designs intended to optimize the features observed from experiments performed to date.

## ACKNOWLEDGMENTS

The authors sincerely thank the NIF operations staff who supported this work. This work was performed under the auspices of the U.S. Department of Energy by Lawrence Livermore National Laboratory under Contract No. DE-AC52-07NA27344 and by General Atomics under Contract No. DE-NA0001808.

[1]J. D. Lindl, *Inertial Confinement Fusion: The Quest for Ignition and Energy Gain Using Indirect Drive* (Springer, New York, NY, USA, 1998).
[2]S. Atzeni and J. Meyer-ter-Vehn, *The Physics of Inertial Fusion* (Oxford University Press, Oxford, 2004).
[3]E. I. Moses, IEEE Trans. Plasma Sci. **38**(4), 684–689 (2010).
[4]S. W. Haan, J. D. Lindl, D. A. Callahan, D. S. Clark, J. D. Salmonson, B. A. Hammel, L. J. Atherton, R. C. Cook, M. J. Edwards, S. Glenzer, A. V. Hamza, S. P. Hatchett, M. C. Herrmann, D. E. Hinkel, D. D. Ho, H. Huang, O. S. Jones, J. Kline, G. Kyrala, O. L. Landen, B. J. MacGowan, M. M. Marinak, D. D. Meyerhofer, J. L. Milovich, K. A. Moreno, E. I. Moses, D. H. Munro, A. Nikroo, R. E. Olson, K. Peterson, S. M. Pollaine, J. E. Ralph, H. F. Robey, B. K. Spears, P. T. Springer, L. J. Suter, C. A. Thomas, R. P. Town, R. Vesey, S. V. Weber, H. L. Wilkens, and D. C. Wilson, Phys. Plasmas **18**(5), 051001 (2011).
[5]M. J. Edwards, J. D. Lindl, B. K. Spears, S. V. Weber, L. J. Atherton, D. L. Bleuel, D. K. Bradley, D. A. Callahan, C. J. Cerjan, D. Clark, G. W. Collins, J. E. Fair, R. J. Fortner, S. H. Glenzer, S. W. Haan, B. A. Hammel, A. V. Hamza, S. P. Hatchett, N. Izumi, B. Jacoby, O. S. Jones, J. A. Koch, B. J. Kozioziemski, O. L. Landen, R. Lerche, B. J. MacGowan, A. J. MacKinnon, E. R. Mapoles, M. M. Marinak, M. Moran, E. I. Moses, D. H. Munro, D. H. Schneider, S. M. Sepke, D. A. Shaughnessy, P. T. Springer, R. Tommasini, L. Bernstein, W. Stoeffl, R. Betti, T. R. Boehly, T. C. Sangster, V. Y. Glebov, P. W. McKenty, S. P. Regan, D. H. Edgell, J. P. Knauer, C. Stoeckl, D. R. Harding, S. Batha, G. Grim, H. W. Herrmann, G. Kyrala, M. Wilke, D. C. Wilson, J. Frenje, R. Petrasso, K. Moreno, H. Huang, K. C. Chen, E. Giraldez, J. D. Kilkenny, M. Mauldin, N. Hein, M. Hoppe, A. Nikroo, and R. J. Leeper, Phys. Plasmas **18**(5), 051003 (2011).
[6]J. Lindl, O. Landen, J. Edwards, E. Moses, and N. Team, Phys. Plasmas **21**(2), 020501 (2014).
[7]J. D. Lindl, O. L. Landen, J. Edwards, E. I. Moses, J. Adams, P. A. Amendt, N. Antipa, P. A. Arnold, L. J. Atherton, S. Azevedo, D. Barker, M. A. Barrios, I. Bass, S. H. Baxamusa, R. Beeler, B. V. Beeman, P. M. Bell, L. R. Benedetti, L. Bernstein, L. Berzak Hopkins, S. D. Bhandarkar, T. Biesiada, R. M. Bionta, D. L. Bleuel, E. J. Bond, M. Borden, M. W. Bowers, D. K. Bradley, D. Browning, G. K. Brunton, J. Bude, S. C. Burkhart, R. F. Burr, B. Butlin, J. A. Caggiano, D. A. Callahan, A. C. Carpenter, C. W. Carr, D. T. Casey, C. Castro, J. Celeste, P. M. Celliers, C. J. Cerjan, J. Chang, M. Chiarappa-Zucca, C. Choate, T. J. Clancy, D. S. Clark, S. J. Cohen, G. W. Collins, A. Conder, J. R. Cox, P. S. Datte, G. A. Deis, E. L. Dewald, P. Di Nicola, J. M. Di Nicola, L. Divol, S. N. Dixit, T. Döppner, V. Draggoo, O. Drury, R. Dylla-Spears, E. G. Dzenitis, J. M. Dzenitis, M. J. Eckart, D. C. Eder, J. H. Eggert, R. B. Ehrlich, G. V. Erbert, J. Fair, D. R. Farley, M. Fedorov, B. Felker, R. Finucane, A. Fisher, D. N. Fittinghoff, J. Folta, R. J. Fortner, T. Frazier, G. Frieders, S. Frieders, S. Friedrich, J. Fry, J. Gaylord, S. M. Glenn, S. H. Glenzer, B. Golick, G. Gururangan, G. Guss, S. W. Haan, B. J. Haid, B. Hammel, A. V. Hamza, E. P. Hartouni, R. Hatarik, B. W. Hatch, S. P. Hatchett, R. Hawley, C. Haynam, J. Heebner, G. Heestand, M. R. Hermann, V. J. Hernandez, D. G. Hicks, D. E. Hinkel, D. D. Ho, J. P. Holder, D. Holunga, J. Honig, J. Horner, R. K. House, M. Hutton, N. Izumi, M. C. Jackson, K. S. Jancaitis, D. R. Jedlovec, M. A. Johnson, O. S. Jones, D. H. Kalantar, R. L. Kauffman, L. Kegelmeyer, G. Kerbel, M. Key, S. F. Khan, J. R. Kimbrough, R. Kirkwood, J. J. Klingman, J. A. Koch, T. R. Kohut, J. M. Koning, K. M. Knittel, B. J. Kozioziemski, G. W. Krauter, K. Krauter, A. Kritcher, J. Kroll, W. L. Kruer, G. LaCaille, K. N. LaFortune, L. J. Lagin, T. A. Land, A. B. Langdon, S. H. Langer, D. W. Larson, D. A. Latray, T. Laurence, S. LePape, R. A. Lerche, Z. Liao, J. Liebman, R. A. London, R. R. Lowe-Webb, T. Ma, B. J. MacGowan, A. J. MacKinnon, A. G. MacPhee, T. N. Malsbury, K. Manes, A. M. Manuel, E. R. Mapoles, M. M. Marinak, C. D. Marshall, D. Mason, N. Masters, D. G. Mathisen, I. Matthews, T. McCarville, J. M. McNaney, D. J. Meeker, N. B. Meezan, J. Menapace, P. Michel, P. E. Miller, J. L. Milovich, M. Mintz, R. Montesanti, M. Monticelli, J. D. Moody, M. J. Moran, J. C. Moreno, D. H. Munro, R. A. Negres, J. R. Nelson, M. Norton, M. Nostrand, M. O'Brien, Y. P. Opachich, C. Orth, A. E. Pak, E. S. Palma, J. N. E. Palmer, T. G. Parham, H.-S. Park, P. K. Patel, R. W. Patterson, J. E. Peterson, J. L. Peterson, T. Phillips, R. Prasad, K. Primdahl, S. T. Prisbrey, S. R. Qiu, J. E. Ralph, K. S. Raman, F. Ravizza, B. Raymond, B. A. Remington, M. A. Rever, J. Reynolds, M. J. Richardson, A. C. Riddle, B. Rittmann, M. D. Rosen, J. S. Ross, J. R. Rygg, R. A. Sacks, J. T. Salmon, J. D. Salmonson, J. D. Sater, R. L. Saunders, R. Sawicki, K. Schaffers, D. H. Schneider, M. B. Schneider, H. A. Scott, S. M. Sepke, R. Seugling, D. A. Shaughnessy, M. J. Shaw, R. Shelton, N. Shen, N. Shingleton, N. Simanovskaia, V. Smalyuk, D. A. Smauley, M. Spaeth, B. K. Spears, D. R. Speck, T. M. Spinka, P. T. Springer, M. Stadermann, W. Stoeffl, J. Stolken, C. Stolz, E. Storm, D. J. Strozzi, T. Suratwala, L. J. Suter, J. S. Taylor, C. A. Thomas, G. L. Tietbohl, R. Tommasini, D. Trummer, B. VanWonterghem, R. Von Rotz, R. J. Wallace, C. F. Walters, A. Wang, A. L. Warrick, S. Weaver, S. V. Weber, P. J. Wegner, K. Widmann, C. C. Widmayer, E. A. Williams, P. K. Whitman, K. Wilhelmsen, M. Witte, L. Wong, R. D. Wood, S. Yang, C. Yeamans, B. K. Young, B. Yoxall, R. A. Zacharias, G. B. Zimmerman, S. Batha, C. R. Danly, V. Fatherley, G. P. Grim, N. Guler, H. W. Herrmann, Y. Kim, J. L. Kline, G. A. Kyrala, R. J. Leeper, D. Martinson, F. E. Merrill, R. E. Olson, C. Wilde, M. D. Wilke, D. C. Wilson, G. A. Chandler, G. W. Cooper, K. D. Hahn, K. J. Peterson, C. L. Ruiz, K. C. Chen, N. Dorsano, M. Emerich, C. Gibson, D. Hoover, M. Hoppe, J. D. Kilkenny, K. Moreno, H. Wilkens, S. Woods, J. A. Frenje, M. G. Johnson, C. K. Li, R. D. Petrasso, H. Rinderknecht, M. Rosenberg, F. H. Séguin, A. Zylstra, W. Garbett, P. Graham, T. Guymer, A. S. Moore, J.-L. Bourgade, P. Gauthier, J.-P. Leidinger, L. Masse, F. Philippe, and R. H. H. Scott, Phys. Plasmas **21**(12), 129902 (2014).
[8]T. Ma, P. K. Patel, N. Izumi, P. T. Springer, M. H. Key, L. J. Atherton, M. A. Barrios, L. R. Benedetti, R. Bionta, E. Bond, D. K. Bradley, J. Caggiano, D. A. Callahan, D. T. Casey, P. M. Celliers, C. J. Cerjan, J. A. Church, D. S. Clark, E. L. Dewald, T. R. Dittrich, S. N. Dixit, T. Döppner, R. Dylla-Spears, D. H. Edgell, R. Epstein, J. Field, D. N. Fittinghoff, J. A. Frenje, M. Gatu Johnson, S. Glenn, S. H. Glenzer, G. Grim, N. Guler, S. W. Haan, B. A. Hammel, R. Hatarik, H. W. Herrmann, D. Hicks, D. E. Hinkel, L. F. Berzak Hopkins, W. W. Hsing, O. A. Hurricane, O. S. Jones, R. Kauffman, S. F. Khan, J. D. Kilkenny, J. L. Kline, B. Kozioziemski, A. Kritcher, G. A. Kyrala, O. L. Landen, J. D. Lindl, S. Le Pape, B. J. MacGowan, A. J. Mackinnon, A. G. MacPhee, N. B. Meezan, F. E. Merrill, J. D. Moody, E. I. Moses, S. R. Nagel, A. Nikroo, A. Pak, T. Parham, H. S. Park, J. E. Ralph, S. P. Regan, B. A. Remington, H. F. Robey, M. D. Rosen, J. R. Rygg, J. S. Ross, J. D. Salmonson, J. Sater, D. Sayre, M. B. Schneider, D. Shaughnessy, H. Sio, B. K. Spears, V. Smalyuk, L. J. Suter, R. Tommasini, R. P. J. Town, P. L. Volegov, A. Wan, S. V. Weber, K. Widmann, C. H. Wilde, C. Yeamans, and M. J. Edwards, Phys. Plasmas **24**(5), 056311 (2017).
[9]O. A. Hurricane, A. Kritcher, D. A. Callahan, O. Landen, P. K. Patel, P. T. Springer, D. T. Casey, E. L. Dewald, T. R. Dittrich, T. Döppner, D. E. Hinkel, L. F. Berzak Hopkins, J. Kline, S. Le Pape, T. Ma, A. G. MacPhee, A. Moore, A. Pak, H. S. Park, J. Ralph, J. D. Salmonson, and K. Widmann, Phys. Plasmas **24**(9), 092706 (2017).
[10]O. A. Hurricane, D. A. Callahan, D. T. Casey, E. L. Dewald, T. R. Dittrich, T. Doppner, S. Haan, D. E. Hinkel, L. F. Berzak Hopkins, O. Jones, A. L. Kritcher, S. Le Pape, T. Ma, A. G. MacPhee, J. L. Milovich, J. Moody, A. Pak, H. S. Park, P. K. Patel, J. E. Ralph, H. F. Robey, J. S. Ross, J. D. Salmonson, B. K. Spears, P. T. Springer, R. Tommasini, F. Albert, L. R. Benedetti, R. Bionta, E. Bond, D. K. Bradley, J. Caggiano, P. M. Celliers, C. Cerjan, J. A. Church, R. Dylla-Spears, D. Edgell, M. J. Edwards, D. Fittinghoff, M. A. Barrios Garcia, A. Hamza, R. Hatarik, H. Herrmann, M. Hohenberger, D. Hoover, J. L. Kline, G. Kyrala, B. Kozioziemski, G. Grim, J. E. Field, J. Frenje, N. Izumi, M. Gatu Johnson, S. F. Khan, J. Knauer, T. Kohut, O. Landen, F. Merrill, P. Michel, A. Moore, S. R. Nagel, A. Nikroo, T. Parham, R. R. Rygg, D. Sayre, M. Schneider, D. Shaughnessy, D. Strozzi, R. P. J. Town, D. Turnbull, P. Volegov, A. Wan, K. Widmann, C. Wilde, and C. Yeamans, Nat. Phys. **12**, 800–806 (2016).
[11]D. A. Callahan *et al.*, "Exploring the limits of case-to-capsule ratio, pulse length, and picket energy for symmetric hohlraum drive on the National Ignition Facility Laser," Phys. Plasmas (to be published).
[12]O. A. Hurricane, D. A. Callahan, D. T. Casey, P. M. Celliers, C. Cerjan, E. L. Dewald, T. R. Dittrich, T. Doppner, D. E. Hinkel, L. F. B. Hopkins, J. L. Kline, S. Le Pape, T. Ma, A. G. MacPhee, J. L. Milovich, A. Pak, H. S. Park, P. K. Patel, B. A. Remington, J. D. Salmonson, P. T. Springer, and R. Tommasini, Nature **506**(7488), 343–348 (2014).
[13]D. T. Casey, J. L. Milovich, V. A. Smalyuk, D. S. Clark, H. F. Robey, A. Pak, A. G. MacPhee, K. L. Baker, C. R. Weber, T. Ma, H. S. Park, T. Döppner, D. A. Callahan, S. W. Haan, P. K. Patel, J. L. Peterson, D. Hoover, A. Nikroo, C. B. Yeamans, F. E. Merrill, P. L. Volegov, D. N. Fittinghoff, G. P. Grim, M. J. Edwards, O. L. Landen, K. N. Lafortune, B. J. MacGowan, C. C. Widmayer, D. B. Sayre, R. Hatarik, E. J. Bond, S. R. Nagel, L. R. Benedetti, N. Izumi, S. Khan, B. Bachmann, B. K. Spears, C. J. Cerjan, M. Gatu Johnson, and J. A. Frenje, Phys. Rev. Lett. **115**(10), 105001 (2015).
[14]C. A. Thomas, Bull. Am. Phys. Soc. **61**, 18 (2016).

[15]K. L. Baker, C. A. Thomas, D. T. Casey, S. Khan, B. K. Spears, R. Nora, T. Woods, J. L. Milovich, R. L. Berger, D. Strozzi, D. Clark, M. Hohenberger, O. A. Hurricane, D. A. Callahan, O. L. Landen, B. Bachmann, R. Benedetti, R. Bionta, P. M. Celliers, D. Fittinghoff, C. Goyon, G. Grim, R. Hatarik, N. Izumi, M. G. Johnson, G. Kyrala, T. Ma, M. Millot, S. R. Nagel, A. Pak, P. K. Patel, D. Turnbull, P. L. Volegov, and C. Yeamans, "High performance indirect-drive cryogenic implosions starting at high adiabat at the National Ignition Facility," (in preparation).

[16]J. D. Moody, P. Michel, L. Divol, R. L. Berger, E. Bond, D. K. Bradley, D. A. Callahan, E. L. Dewald, S. Dixit, M. J. Edwards, S. Glenn, A. Hamza, C. Haynam, D. E. Hinkel, N. Izumi, O. Jones, J. D. Kilkenny, R. K. Kirkwood, J. L. Kline, W. L. Kruer, G. A. Kyrala, O. L. Landen, S. LePape, J. D. Lindl, B. J. MacGowan, N. B. Meezan, A. Nikroo, M. D. Rosen, M. B. Schneider, D. J. Strozzi, L. J. Suter, C. A. Thomas, R. P. J. Town, K. Widmann, E. A. Williams, L. J. Atherton, S. H. Glenzer, and E. I. Moses, Nat. Phys. **8**(4), 344–349 (2012).

[17]G. N. Hall, O. S. Jones, D. J. Strozzi, J. D. Moody, D. Turnbull, J. Ralph, P. A. Michel, M. Hohenberger, A. S. Moore, O. L. Landen, L. Divol, D. K. Bradley, D. E. Hinkel, A. J. Mackinnon, R. P. J. Town, N. B. Meezan, L. Berzak Hopkins, and N. Izumi, Phys. Plasmas **24**(5), 052706 (2017).

[18]D. S. Clark, A. L. Kritcher, S. A. Yi, A. B. Zylstra, S. W. Haan, and C. R. Weber, "Capsule physics comparison of National Ignition Facility implosion design using plastic, diamond, and beryllium ablators," Phys. Plasmas (to be published).

[19]J. E. Ralph, A. Pak, O. Landen, T. Ma, D. A. Callahan, A. Kritcher, L. Divol, T. Döppner, D. E. Hinkel, C. Jarrott, J. D. Moody, B. B. Pollock, O. Hurricane, and A. J. Edwards, "Hohlraum dynamics influence on implosion symmetry in indirect drive inertial confinement fusion experiments," (in preparation).

[20]P. Amendt, J. S. Ross, J. L. Milovich, M. Schneider, E. Storm, D. A. Callahan, D. Hinkel, B. Lasinski, D. Meeker, P. Michel, J. Moody, and D. Strozzi, Phys. Plasmas **21**(11), 112703 (2014).

[21]D. D. Ho, Bull. Am. Phys. Soc. **52**(16), 273 (2007).

[22]A. J. MacKinnon, N. B. Meezan, J. S. Ross, S. Le Pape, L. Berzak Hopkins, L. Divol, D. Ho, J. Milovich, A. Pak, J. Ralph, T. Döppner, P. K. Patel, C. Thomas, R. Tommasini, S. Haan, A. G. MacPhee, J. McNaney, J. Caggiano, R. Hatarik, R. Bionta, T. Ma, B. Spears, J. R. Rygg, L. R. Benedetti, R. P. J. Town, D. K. Bradley, E. L. Dewald, D. Fittinghoff, O. S. Jones, H. R. Robey, J. D. Moody, S. Khan, D. A. Callahan, A. Hamza, J. Biener, P. M. Celliers, D. G. Braun, D. J. Erskine, S. T. Prisbrey, R. J. Wallace, B. Kozioziemski, R. Dylla-Spears, J. Sater, G. Collins, E. Storm, W. Hsing, O. Landen, J. L. Atherton, J. D. Lindl, M. J. Edwards, J. A. Frenje, M. Gatu-Johnson, C. K. Li, R. Petrasso, H. Rinderknecht, M. Rosenberg, F. H. Séguin, A. Zylstra, J. P. Knauer, G. Grim, N. Guler, F. Merrill, R. Olson, G. A. Kyrala, J. D. Kilkenny, A. Nikroo, K. Moreno, D. E. Hoover, C. Wild, and E. Werner, Phys. Plasmas (1994-present) **21**(5), 056318 (2014).

[23]J. S. Ross, D. Ho, J. Milovich, T. Döppner, J. McNaney, A. G. MacPhee, A. Hamza, J. Biener, H. F. Robey, E. L. Dewald, R. Tommasini, L. Divol, S. Le Pape, L. B. Hopkins, P. M. Celliers, O. Landen, N. B. Meezan, and A. J. Mackinnon, Phys. Rev. E **91**(2), 021101 (2015).

[24]L. F. Berzak Hopkins, N. B. Meezan, S. Le Pape, L. Divol, A. J. Mackinnon, D. D. Ho, M. Hohenberger, O. S. Jones, G. Kyrala, J. L. Milovich, A. Pak, J. E. Ralph, J. S. Ross, L. R. Benedetti, J. Biener, R. Bionta, E. Bond, D. Bradley, J. Caggiano, D. Callahan, C. Cerjan, J. Church, D. Clark, T. Döppner, R. Dylla-Spears, M. Eckart, D. Edgell, J. Field, D. N. Fittinghoff, M. Gatu Johnson, G. Grim, N. Guler, S. Haan, A. Hamza, E. P. Hartouni, R. Hatarik, H. W. Herrmann, D. Hinkel, D. Hoover, H. Huang, N. Izumi, S. Khan, B. Kozioziemski, J. Kroll, T. Ma, A. MacPhee, J. McNaney, F. Merrill, J. Moody, A. Nikroo, P. Patel, H. F. Robey, J. R. Rygg, J. Sater, D. Sayre, M. Schneider, S. Sepke, M. Stadermann, W. Stoeffl, C. Thomas, R. P. J. Town, P. L. Volegov, C. Wild, C. Wilde, E. Woerner, C. Yeamans, B. Yoxall, J. Kilkenny, O. L. Landen, W. Hsing, and M. J. Edwards, Phys. Rev. Lett. **114**(17), 175001 (2015).

[25]D. D. M. Ho, S. W. Haan, J. D. Salmonson, D. S. Clark, J. D. Lindl, J. L. Milovich, C. A. Thomas, L. F. B. Hopkins, and N. B. Meezan, J. Phys.: Conf. Ser. **717**(1), 012023 (2016).

[26]N. B. Meezan, L. F. Berzak Hopkins, S. Le Pape, L. Divol, A. J. MacKinnon, T. Döppner, D. D. Ho, O. S. Jones, S. F. Khan, T. Ma, J. L. Milovich, A. E. Pak, J. S. Ross, C. A. Thomas, L. R. Benedetti, D. K. Bradley, P. M. Celliers, D. S. Clark, J. E. Field, S. W. Haan, N. Izumi, G. A. Kyrala, J. D. Moody, P. K. Patel, J. E. Ralph, J. R. Rygg, S. M. Sepke, B. K. Spears, R. Tommasini, R. P. J. Town, J. Biener, R. M. Bionta, E. J. Bond, J. A. Caggiano, M. J. Eckart, M. Gatu Johnson, G. P. Grim, A. V. Hamza, E. P. Hartouni, R. Hatarik, D. E. Hoover, J. D. Kilkenny, B. J. Kozioziemski, J. J. Kroll, J. M. McNaney, A. Nikroo, D. B. Sayre, M. Stadermann, C. Wild, B. E. Yoxall, O. L. Landen, W. W. Hsing, and M. J. Edwards, Phys. Plasmas **22**(6), 062703 (2015).

[27]L. Divol, A. Pak, L. F. Berzak Hopkins, S. Le Pape, N. B. Meezan, E. L. Dewald, D. D. M. Ho, S. F. Khan, A. J. Mackinnon, J. S. Ross, D. P. Turnbull, C. Weber, P. M. Celliers, M. Millot, L. R. Benedetti, J. E. Field, N. Izumi, G. A. Kyrala, T. Ma, S. R. Nagel, J. R. Rygg, D. Edgell, A. G. Macphee, C. Goyon, M. Hohenberger, B. J. MacGowan, P. Michel, D. Strozzi, W. Cassata, D. Casey, D. N. Fittinghoff, N. Gharibyan, R. Hatarik, D. Sayre, P. Volegov, C. Yeamans, B. Bachmann, T. Döppner, J. Biener, J. Crippen, C. Choate, H. Huang, C. Kong, A. Nikroo, N. G. Rice, M. Stadermann, S. D. Bhandarkar, S. Haan, B. Kozioziemski, W. W. Hsing, O. L. Landen, J. D. Moody, R. P. J. Town, D. A. Callahan, O. A. Hurricane, and M. J. Edwards, Phys. Plasmas **24**(5), 056309 (2017).

[28]L. F. Berzak Hopkins, S. Le Pape, L. Divol, N. B. Meezan, A. J. Mackinnon, D. D. Ho, O. S. Jones, S. Khan, J. L. Milovich, J. S. Ross, P. Amendt, D. Casey, P. M. Celliers, A. Pak, J. L. Peterson, J. Ralph, and J. R. Rygg, Phys. Plasmas **22**(5), 056318 (2015).

[29]J. Biener, D. D. Ho, S. Kucheyev, Y.-M. Wang, J. Ye, N. E. T. C. K. Saw, Jr., T. Braun, H. Huang, W. Requieron, S. W. Haan, N. B. Meezan, M. Stadermann, A. Nikroo, A. V. Hamza, and C. Wild (unpublished).

[30]G. A. Kyrala, J. L. Kline, S. Dixit, S. Glenzer, D. Kalantar, D. Bradley, N. Izumi, N. Meezan, O. Landen, D. Callahan, S. V. Weber, J. P. Holder, S. Glenn, M. J. Edwards, J. Koch, L. J. Suter, S. W. Haan, R. P. J. Town, P. Michel, O. Jones, S. Langer, J. D. Moody, E. L. Dewald, T. Ma, J. Ralph, A. Hamza, E. Dzenitis, and J. Kilkenny, Phys. Plasmas **18**(5), 056307 (2011).

[31]S. M. Glenn, L. R. Benedetti, D. K. Bradley, B. A. Hammel, N. Izumi, S. F. Khan, G. A. Kyrala, T. Ma, J. L. Milovich, A. E. Pak, V. A. Smalyuk, R. Tommasini, and R. P. Town, Rev. Sci. Instrum. **83**(10), 10E519 (2012).

[32]T. Ma, N. Izumi, R. Tommasini, D. K. Bradley, P. Bell, C. J. Cerjan, S. Dixit, T. Döppner, O. Jones, J. L. Kline, G. Kyrala, O. L. Landen, S. LePape, A. J. Mackinnon, H. S. Park, P. K. Patel, R. R. Prasad, J. Ralph, S. P. Regan, V. A. Smalyuk, P. T. Springer, L. Suter, R. P. J. Town, S. V. Weber, and S. H. Glenzer, Rev. Sci. Instrum. **83**(10), 10E115 (2012).

[33]M. C. Herrmann, M. Tabak, and J. D. Lindl, Nucl. Fusion **41**(1), 99 (2001).

[34]C. D. Zhou and R. Betti, Phys. Plasmas **15**(10), 102707–102712 (2008).

[35]R. Nora, R. Betti, K. S. Anderson, A. Shvydky, A. Bose, K. M. Woo, A. R. Christopherson, J. A. Marozas, T. J. B. Collins, P. B. Radha, S. X. Hu, R. Epstein, F. J. Marshall, R. L. McCrory, T. C. Sangster, and D. D. Meyerhofer, Phys. Plasmas **21**(5), 056316 (2014).

[36]R. P. Drake, *High-Energy-Density Physics: Fundamentals, Inertial Fusion, and Experimental Astrophysics* (Springer, 2006).

[37]D. Ryutov, R. P. Drake, J. Kane, E. Liang, B. A. Remington, and W. M. Wood-Vasey, Astrophys. J. **518**(2), 821 (1999).

[38]S. R. Nagel, S. W. Haan, J. R. Rygg, M. Barrios, L. R. Benedetti, D. K. Bradley, J. E. Field, B. A. Hammel, N. Izumi, O. S. Jones, S. F. Khan, T. Ma, A. E. Pak, R. Tommasini, and R. P. J. Town, Phys. Plasmas (1994-present) **22**(2), 022704 (2015).

[39]A. G. MacPhee, D. T. Casey, D. S. Clark, S. Felker, J. E. Field, S. W. Haan, B. A. Hammel, J. Kroll, O. L. Landen, D. A. Martinez, P. Michel, J. Milovich, A. Moore, A. Nikroo, N. Rice, H. F. Robey, V. A. Smalyuk, M. Stadermann, and C. R. Weber, Phys. Rev. E **95**(3), 031204 (2017).

[40]J. A. Koch, B. J. Kozioziemski, J. Salmonson, A. Chernov, L. J. Atherton, E. Dewald, N. Izumi, M. A. Johnson, S. Kucheyev, J. Lugten, E. Mapoles, J. D. Moody, J. W. Pipes, J. D. Sater, and D. Stefanescu, Fusion Sci. Technol. **55**(3), 244–252 (2009).

[41]B. K. Spears, S. Glenzer, M. J. Edwards, S. Brandon, D. Clark, R. Town, C. Cerjan, R. Dylla-Spears, E. Mapoles, D. Munro, J. Salmonson, S. Sepke, S. Weber, S. Hatchett, S. Haan, P. Springer, E. Moses, J. Kline, G. Kyrala, and D. Wilson, Phys. Plasmas **19**(5), 056316 (2012).

[42]H.-S. Park, B. R. Maddox, E. Giraldez, S. P. Hatchett, L. T. Hudson, N. Izumi, M. H. Key, S. L. Pape, A. J. MacKinnon, A. G. MacPhee, P. K. Patel, T. W. Phillips, B. A. Remington, J. F. Seely, R. Tommasini, R. Town, J. Workman, and E. Brambrink, Phys. Plasmas **15**(7), 072705 (2008).

[43]A. Pak (unpublished).

[44]R. Betti, A. R. Christopherson, B. K. Spears, R. Nora, A. Bose, J. Howard, K. M. Woo, M. J. Edwards, and J. Sanz, Phys. Rev. Lett. **114**(25), 255003 (2015).

[45]V. A. Smalyuk, H. F. Robey, T. Döppner, D. T. Casey, D. S. Clark, O. S. Jones, J. L. Milovich, J. L. Peterson, B. Bachmann, K. L. Baker, L. R. Benedetti, L. F. Berzak Hopkins, R. Bionta, E. Bond, D. K. Bradley, D. A. Callahan, P. M. Celliers, C. Cerjan, K. C. Chen, C. Goyon, G. Grim, S. N. Dixit, M. J. Eckart, M. J. Edwards, M. Farrell, D. N. Fittinghoff, J. A. Frenje, M. Gatu-Johnson, N. Gharibyan, S. W. Haan, A. V. Hamza, E. Hartouni, R. Hatarik, M. Havre, M. Hohenberger, D. Hoover, O. A. Hurricane, N. Izumi, K. S. Jancaitis, S. F. Khan, J. P. Knauer, J. J. Kroll, G. Kyrala, K. N. Lafortune, O. L. Landen, T. Ma, B. J. MacGowan, A. G. MacPhee, M. Mauldin, F. E. Merrill, A. S. Moore, S. Nagel, A. Nikroo, A. Pak, P. K. Patel, J. E. Ralph, D. B. Sayre, D. Shaughnessy, B. K. Spears, R. Tommasini, D. P. Turnbull, A. L. Velikovich, P. L. Volegov, C. R. Weber, C. C. Widmayer, and C. Yeamans, Phys. Plasmas **23**(10), 102703 (2016).

[46]B. Spears, Bull. Am. Phys. Soc. **61**, 18 (2016).

[47]P. Y. Chang, R. Betti, B. K. Spears, K. S. Anderson, J. Edwards, M. Fatenejad, J. D. Lindl, R. L. McCrory, R. Nora, and D. Shvarts, Phys. Rev. Lett. **104**(13), 135002 (2010).

[48]R. Tipton, in Proceedings of the IFSA (2015).

[49]R. Betti, P. Y. Chang, B. K. Spears, K. S. Anderson, J. Edwards, M. Fatenejad, J. D. Lindl, R. L. McCrory, R. Nora, and D. Shvarts, Phys. Plasmas **17**(5), 058102 (2010).

[50]G. P. Grim, N. Guler, F. E. Merrill, G. L. Morgan, C. R. Danly, P. L. Volegov, C. H. Wilde, D. C. Wilson, D. S. Clark, D. E. Hinkel, O. S. Jones, K. S. Raman, N. Izumi, D. N. Fittinghoff, O. B. Drury, E. T. Alger, P. A. Arnold, R. C. Ashabranner, L. J. Atherton, M. A. Barrios, S. Batha, P. M. Bell, L. R. Benedetti, R. L. Berger, L. A. Bernstein, L. V. Berzins, R. Betti, S. D. Bhandarkar, R. M. Bionta, D. L. Bleuel, T. R. Boehly, E. J. Bond, M. W. Bowers, D. K. Bradley, G. K. Brunton, R. A. Buckles, S. C. Burkhart, R. F. Burr, J. A. Caggiano, D. A. Callahan, D. T. Casey, C. Castro, P. M. Celliers, C. J. Cerjan, G. A. Chandler, C. Choate, S. J. Cohen, G. W. Collins, G. W. Cooper, J. R. Cox, J. R. Cradick, P. S. Datte, E. L. Dewald, P. D. Nicola, J. M. D. Nicola, L. Divol, S. N. Dixit, R. Dylla-Spears, E. G. Dzenitis, M. J. Eckart, D. C. Eder, D. H. Edgell, M. J. Edwards, J. H. Eggert, R. B. Ehrlich, G. V. Erbert, J. Fair, D. R. Farley, B. Felker, R. J. Fortner, J. A. Frenje, G. Frieders, S. Friedrich, M. Gatu-Johnson, C. R. Gibson, E. Giraldez, V. Y. Glebov, S. M. Glenn, S. H. Glenzer, G. Gururangan, S. W. Haan, K. D. Hahn, B. A. Hammel, A. V. Hamza, E. P. Hartouni, R. Hatarik, S. P. Hatchett, C. Haynam, M. R. Hermann, H. W. Herrmann, D. G. Hicks, J. P. Holder, D. M. Holunga, J. B. Horner, W. W. Hsing, H. Huang, M. C. Jackson, K. S. Jancaitis, D. H. Kalantar, R. L. Kauffman, M. I. Kauffman, S. F. Khan, J. D. Kilkenny, J. R. Kimbrough, R. Kirkwood, J. L. Kline, J. P. Knauer, K. M. Knittel, J. A. Koch, T. R. Kohut, B. J. Kozioziemski, K. Krauter, G. W. Krauter, A. L. Kritcher, J. Kroll, G. A. Kyrala, K. N. L. Fortune, G. LaCaille, L. J. Lagin, T. A. Land, O. L. Landen, D. W. Larson, D. A. Latray, R. J. Leeper, T. L. Lewis, S. LePape, J. D. Lindl, R. R. Lowe-Webb, T. Ma, B. J. MacGowan, A. J. MacKinnon, A. G. MacPhee, R. M. Malone, T. N. Malsbury, E. Mapoles, C. D. Marshall, D. G. Mathisen, P. McKenty, J. M. McNaney, N. B. Meezan, P. Michel, J. L. Milovich, J. D. Moody, A. S. Moore, M. J. Moran, K. Moreno, E. I. Moses, D. H. Munro, B. R. Nathan, A. J. Nelson, A. Nikroo, R. E. Olson, C. Orth, A. E. Pak, E. S. Palma, T. G. Parham, P. K. Patel, R. W. Patterson, R. D. Petrasso, R. Prasad, J. E. Ralph, S. P. Regan, H. Rinderknecht, H. F. Robey, G. F. Ross, C. L. Ruiz, F. H. Seguin, J. D. Salmonson, T. C. Sangster, J. D. Sater, R. L. Saunders, M. B. Schneider, D. H. Schneider, M. J. Shaw, N. Simanovskaia, B. K. Spears, P. T. Springer, C. Stoeckl, W. Stoeffl, L. J. Suter, C. A. Thomas, R. Tommasini, R. P. Town, A. J. Traille, B. V. Wonterghem, R. J. Wallace, S. Weaver, S. V. Weber, P. J. Wegner, P. K. Whitman, K. Widmann, C. C. Widmayer, R. D. Wood, B. K. Young, R. A. Zacharias, and A. Zylstra, Phys. Plasmas **20**(5), 056320 (2013).

[51]P. Volegov, C. R. Danly, D. N. Fittinghoff, G. P. Grim, N. Guler, N. Izumi, T. Ma, F. E. Merrill, A. L. Warrick, C. H. Wilde, and D. C. Wilson, Rev. Sci. Instrum. **85**(2), 023508 (2014).

[52]C. B. Yeamans and D. L. Bleuel, Fusion Sci. Technol. **72**(2), 120–128 (2017).

[53]R. Hatarik, D. B. Sayre, J. A. Caggiano, T. Phillips, M. J. Eckart, E. J. Bond, C. Cerjan, G. P. Grim, E. P. Hartouni, J. P. Knauer, J. M. Mcnaney, and D. H. Munro, J. Appl. Phys. **118**(18), 184502 (2015).

[54]M. Gatu Johnson, J. A. Frenje, R. M. Bionta, D. T. Casey, M. J. Eckart, M. P. Farrell, G. P. Grim, E. P. Hartouni, R. Hatarik, M. Hoppe, J. D. Kilkenny, C. K. Li, R. D. Petrasso, H. G. Reynolds, D. B. Sayre, M. E. Schoff, F. H. Séguin, K. Skulina, and C. B. Yeamans, Rev. Sci. Instrum. **87**(11), 11D816 (2016).

[55]M. J. Edwards, P. K. Patel, J. D. Lindl, L. J. Atherton, S. H. Glenzer, S. W. Haan, J. D. Kilkenny, O. L. Landen, E. I. Moses, A. Nikroo, R. Petrasso, T. C. Sangster, P. T. Springer, S. Batha, R. Benedetti, L. Bernstein, R. Betti, D. L. Bleuel, T. R. Boehly, D. K. Bradley, J. A. Caggiano, D. A. Callahan, P. M. Celliers, C. J. Cerjan, K. C. Chen, D. S. Clark, G. W. Collins, E. L. Dewald, L. Divol, S. Dixit, T. Doeppner, D. H. Edgell, J. E. Fair, M. Farrell, R. J. Fortner, J. Frenje, M. G. G. Johnson, E. Giraldez, V. Y. Glebov, G. Grim, B. A. Hammel, A. V. Hamza, D. R. Harding, S. P. Hatchett, N. Hein, H. W. Herrmann, D. Hicks, D. E. Hinkel, M. Hoppe, W. W. Hsing, N. Izumi, B. Jacoby, O. S. Jones, D. Kalantar, R. Kauffman, J. L. Kline, J. P. Knauer, J. A. Koch, B. J. Kozioziemski, G. Kyrala, K. N. LaFortune, S. L. Pape, R. J. Leeper, R. Lerche, T. Ma, B. J. MacGowan, A. J. MacKinnon, A. Macphee, E. R. Mapoles, M. M. Marinak, M. Mauldin, P. W. McKenty, M. Meezan, P. A. Michel, J. Milovich, J. D. Moody, M. Moran, D. H. Munro, C. L. Olson, K. Opachich, A. E. Pak, T. Parham, H.-S. Park, J. E. Ralph, S. P. Regan, B. Remington, H. Rinderknecht, H. F. Robey, M. Rosen, S. Ross, J. D. Salmonson, J. Sater, D. H. Schneider, F. H. Seguin, S. M. Sepke, D. A. Shaughnessy, V. A. Smalyuk, B. K. Spears, C. Stoeckl, W. Stoeffl, L. Suter, C. A. Thomas, R. Tommasini, R. P. Town, S. V. Weber, P. J. Wegner, K. Widman, M. Wilke, D. C. Wilson, C. B. Yeamans, and A. Zylstra, Phys. Plasmas **20**(7), 070501 (2013).

[56]L. B. Hopkins, C. Weber, L. Divol, S. L. Pape, N. B. Meezan, D. D. Ho, A. Pak, E. Dewald, C. Goyon, J. Biener, S. Khan, C. Kong, A. Nikroo, N. Rice, M. Stadermann, R. Tommassini, C. Wild, D. Callahan, and O. Hurricane, "Increased stagnation pressure and performance of ICF capsules with the introduction of a high-Z dopant" (submitted).

[57]H. S. Park, O. A. Hurricane, D. A. Callahan, D. T. Casey, E. L. Dewald, T. R. Dittrich, T. Döppner, D. E. Hinkel, L. F. Berzak Hopkins, S. Le Pape, T. Ma, P. K. Patel, B. A. Remington, H. F. Robey, J. D. Salmonson, and J. L. Kline, Phys. Rev. Lett. **112**(5), 055001 (2014).

[58]S. L. Pape, L. F. B. Hopkins, L. Divol, A. Pak, E. Dewald, N. B. Meezan, D. D.-M. Ho, S. F. Khan, A. J. Mackinnon, C. Weber, C. Goyon, J. S. Ross, J. Ralph, J. Milovich, M. Millot, L. R. Bennedetti, N. Izumi, G. A. Kyrala, T. Ma, S. R. Nagel, D. Edgell, A. G. MacPhee, B. J. MacGowan, P. Michel, D. Strozzi, D. N. Fittinghoff, D. Casey, R. Hatarik, P. Volegov, C. Yeamans, M. Gatu-Johnson, J. Biener, N. G. Rice, M. Stadermann, S. Bhandarkar, S. Haan, P. Patel, D. Callahan, and O. A. Hurricane (submitted).

[59]A. L. Kritcher *et al.*, "Comparison of plastic, diamond, and beryllium as candidate indirect drive NIF Ablators," Phys. Plasmas (to be published).